

Regularization Schemes for Linear Inverse Problems

Haley Rosso & Andreas Mang

Department of Mathematics, University of Houston, Houston, TX, USA

UNIVERSITY of
HOUSTON

Introduction

Teaser: Our primary goal is the design of effective regularization schemes for inverse problems.

Mathematical Problem Formulation

In a first step, we consider linear inverse problems [1]. That is, we assume that the observed data $\mathbf{y}_{\text{obs}} = \mathbf{A}\mathbf{x} + \boldsymbol{\eta}$, where $\mathbf{x} \in \mathbb{R}^n$, $\mathbf{A} \in \mathbb{R}^{m,n}$, $\mathbf{y}_{\text{obs}} \in \mathbb{R}^m$, and $\boldsymbol{\eta} \propto \mathcal{N}(0, \mathbf{I}_n)$ is a random perturbation. In the inverse problem, we seek \mathbf{x} given \mathbf{y}_{obs} and \mathbf{A} . In general, \mathbf{A} will not be invertible and $\mathbf{y}_{\text{obs}} \notin \text{col } \mathbf{A}$. Consequently, we will formulate the solution of the linear system $\mathbf{A}\mathbf{x} = \mathbf{y}_{\text{obs}}$ as a **regularized least squares problem** of the form

$$\underset{\mathbf{x} \in \mathbb{R}^n}{\text{minimize}} \quad f(\mathbf{x}), \quad \text{where } f(\mathbf{x}) := \frac{1}{2} \|\mathbf{A}\mathbf{x} - \mathbf{y}_{\text{obs}}\|_2^2 + \frac{\alpha}{2} \|\mathbf{L}\mathbf{x}\|_2^2. \quad (1)$$

The first term of f measures the discrepancy between the model prediction $\mathbf{A}\mathbf{x} =: \mathbf{y}_{\text{pred}}$ and the observed data \mathbf{y}_{obs} . The second term $\|\mathbf{L}\mathbf{x}\|_2^2 = \langle \mathbf{L}^T \mathbf{L}\mathbf{x}, \mathbf{x} \rangle$, $\mathbf{L} \in \mathbb{R}^{n,n}$, is a **regularization functional**; it is introduced to alleviate mathematical issues with the **ill-posedness** of the inverse problem, with regularization operator \mathbf{L} and regularization parameter $\alpha > 0$. We will see that the choices for \mathbf{L} and α greatly affect the computed solution \mathbf{x} of (1). We consider the following regularization operators: (i) $\mathbf{L}^T \mathbf{L} = \mathbf{I}_n$ (identity matrix), (ii) $\mathbf{L}^T \mathbf{L} = -\Delta$ (Laplace operator), and (iii) $\mathbf{L}^T \mathbf{L} = \mathbf{I}_n - \mathbf{V}\mathbf{V}^T$, where \mathbf{V} are the right-singular values of \mathbf{A} (see below) [2].

Optimality Conditions

For an admissible solution $\mathbf{x}^* \in \mathbb{R}^n$ of (1) we require that the gradient $\nabla f(\mathbf{x}^*)$, $f: \mathbb{R}^n \rightarrow \mathbb{R}$ of the objective function f vanishes. The gradient of f is given by

$$\nabla f(\mathbf{x}) = \nabla \left(\frac{1}{2} \|\mathbf{A}\mathbf{x} - \mathbf{b}\|_2^2 + \frac{\alpha}{2} \|\mathbf{L}\mathbf{x}\|_2^2 \right) = \mathbf{A}^T(\mathbf{A}\mathbf{x} - \mathbf{b}) + \alpha \mathbf{L}^T \mathbf{L}\mathbf{x}.$$

Consequently, at optimality we have

$$\mathbf{A}^T(\mathbf{A}\mathbf{x}^* - \mathbf{b}) + \alpha \mathbf{L}^T \mathbf{L}\mathbf{x}^* \stackrel{!}{=} 0, \quad (2)$$

the so-called normal equation.

Numerical Methods

We consider different approaches to solve $\mathbf{A}\mathbf{x} = \mathbf{y}_{\text{obs}}$ for \mathbf{x} . We consider two classes of approaches—direct solvers and iterative methods.

Direct Solvers

In our first approach, we consider direct solvers for computing a solution to the regularized least squares problem (1). Here, we directly solve the optimality system (2) using MATLAB's backslash command; the numerical solution is given by

$$\mathbf{x}_{\text{sol}} = (\mathbf{A}^T \mathbf{A} + \alpha \mathbf{L}^T \mathbf{L})^{-1} \mathbf{A}^T \mathbf{b}.$$

In our second approach, we compute the pseudo-inverse \mathbf{A}^+ of \mathbf{A} . We use a **truncated singular value decomposition (TSVD)**. That is, we compute the factorization $\mathbf{U}\mathbf{S}\mathbf{V}^T$ of \mathbf{A} , where $\mathbf{U} \in \mathbb{R}^{m,m}$ is an orthogonal matrix for the left-singular vectors, $\mathbf{S} \in \mathbb{R}^{m,n}$ diagonal matrix for the singular values, and $\mathbf{V} \in \mathbb{R}^{n,n}$ is an orthogonal matrix for the right-singular values of \mathbf{A} . Suppose that \mathbf{A} has rank $r \ll n$. Under this assumption, $\mathbf{U} =$

$[\mathbf{u}_1 \dots \mathbf{u}_r \quad \mathbf{u}_{r+1} \dots \mathbf{u}_m] \in \mathbb{R}^{m,m}$, $\mathbf{S} = \text{diag}(\sigma_1, \dots, \sigma_r, 0, \dots, 0) \in \mathbb{R}^{m,n}$, and $\mathbf{V} = [\mathbf{v}_1 \dots \mathbf{v}_r \quad \mathbf{v}_{r+1} \dots \mathbf{v}_n] \in \mathbb{R}^{n,n}$. Consequently, we can decompose \mathbf{A} into

$$\mathbf{A} \approx \mathbf{U}_r \mathbf{S}_r \mathbf{V}_r^T,$$

where $\mathbf{U}_r = [\mathbf{u}_1 \dots \mathbf{u}_r] \in \mathbb{R}^{m,r}$ and $\mathbf{V}_r = [\mathbf{v}_1 \dots \mathbf{v}_r] \in \mathbb{R}^{n,r}$ are the left- and right singular values and $\mathbf{S}_r = \text{diag}(\sigma_1, \dots, \sigma_r) \in \mathbb{R}^{r,r}$. The pseudo-inverse is given by $\mathbf{A}^+ = \mathbf{V}\mathbf{S}^+ \mathbf{U}^T$, where $\mathbf{S}^+ \in \mathbb{R}^{n,m}$ is computed by taking the reciprocal of each non-zero element on the diagonal (leaving the zeros in place) and then transposing the matrix. In numerical computation, we either select a small tolerance $\epsilon > 0$ and set all $\sigma_i \leq \epsilon$ to 0, or we select a target rank r . The choice of the target rank depends on how fast the spectrum decays.

Iterative Solvers

We use an iterative scheme of the form

$$\mathbf{x}_{k+1} = \mathbf{x}_k - \gamma_k \mathbf{B}_k \nabla f(\mathbf{x}_k), \quad k = 1, 2, \dots$$

Here, $k \in \mathbb{N}$ is the iteration index and $\gamma_k \in [0, 1]$ is determined using a backtracking line search [3,4]. The search direction is given by $\mathbf{s}_k := -\mathbf{B}_k \nabla f(\mathbf{x}_k)$. We consider a gradient descent approach for which $\mathbf{B}_k = \mathbf{I}_n$ and Newton's method with $\mathbf{B}_k = (\nabla^2 f(\mathbf{x}_k))^{-1}$, where $\nabla^2 f(\mathbf{x}_k) = \mathbf{A}^T \mathbf{A} + \alpha \mathbf{L}^T \mathbf{L}$ is the Hessian matrix. In our prototype implementation we invert the Hessian matrix using MATLAB's backslash. We terminate our solver if (i) we reach a user defined number of iterations, or (ii) the ℓ^2 -norm of the gradient is reduced by a user defined tolerance $\kappa > 0$, or (iii) the ℓ^2 -norm of $\nabla f(\mathbf{x}_k)$ is smaller or equal to $1\text{e}-6$. Our numerical scheme is as follows.

```
1:  $\mathbf{x}_0 \leftarrow 0, \quad k \leftarrow 0$ 
2:  $\mathbf{g}_0 \leftarrow \text{objfun}(\mathbf{x}_0)$ 
3: while not converged do
4:    $\mathbf{s}_k \leftarrow \text{compSearchDir}(\text{objfun}, \mathbf{x}_k, \mathbf{g}_k)$ 
5:    $\gamma_k \leftarrow \text{doLineSearch}(\text{objfun}, \mathbf{x}_k, \mathbf{s}_k)$ 
6:    $\mathbf{x}_k \leftarrow \mathbf{x}_k + \gamma_k \mathbf{s}_k, \quad k \leftarrow k + 1$ 
7:   converged  $\leftarrow \text{checkConvergence}(k, \mathbf{g}_k, \mathbf{g}_0)$ 
```

Regularization Parameter Selection

To identify an optimal regularization parameter α , we consider the L-curve method [1], i.e., a log-log plot of the norm of a regularized solution versus the norm of the corresponding residual norm.

Numerical Experiments

Synthetic Test Problem

We consider a synthetic test problem to study the performance of the proposed methodology. The operators in (1) are as follows: For \mathbf{A} , we consider a Helmholtz-type operator of the general form $\mathbf{A} = (-\Delta + k^2 \mathbf{I}_n)^{-1}$, where $-\Delta$ is a Laplace operator, $k > 0$, and \mathbf{I}_n is an $n \times n$ identity matrix. The structure of the matrix \mathbf{A} is shown in **Figure 1**.

We compute \mathbf{y}_{obs} by applying the forward operator \mathbf{A} . That is, $\mathbf{y}_{\text{obs}} = \mathbf{A}\mathbf{x}_{\text{true}} + \kappa \boldsymbol{\eta}$, $\boldsymbol{\eta} \propto \mathcal{N}(0, \mathbf{I}_n)$, $\kappa = \theta \|\mathbf{x}_{\text{true}}\|_2^2$, $\theta \in [0, 1]$. We select

$$\mathbf{x}_{\text{true}} := (\sin(\mathbf{z}) + \gamma \mathbf{z} \odot \sin(4\mathbf{z})) \odot \exp(-\|\mathbf{z} - \boldsymbol{\pi}\|_2^2 / 2\kappa), \quad (3)$$

with $\kappa = 9/10$ and $\gamma = 7/2$ and $\mathbf{z}_i = hi$, $h = 2\pi/n$, $i = 1, \dots, n$.

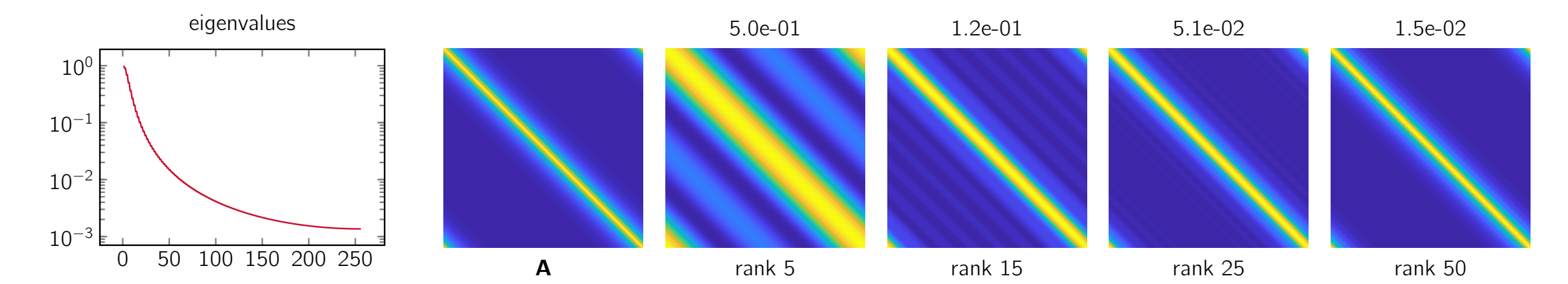


Figure 1: Visualization of the structure of the Helmholtz matrix \mathbf{A} . We show the decay of the eigenvalues on the left. The remaining figures (from left to right) show the entries of the matrix \mathbf{A} and low rank approximations \mathbf{A}_r for $r \in \{5, 15, 25, 50\}$ built using TSVD. Above each visualization of the low rank approximations we report the relative error $\|\mathbf{A} - \mathbf{A}_r\|_F^2 / \|\mathbf{A}\|_F^2$.

Numerical Results

We report numerical results for different strategies to solve the considered inverse problem for the test problem described in the former section in **Figure 2**.

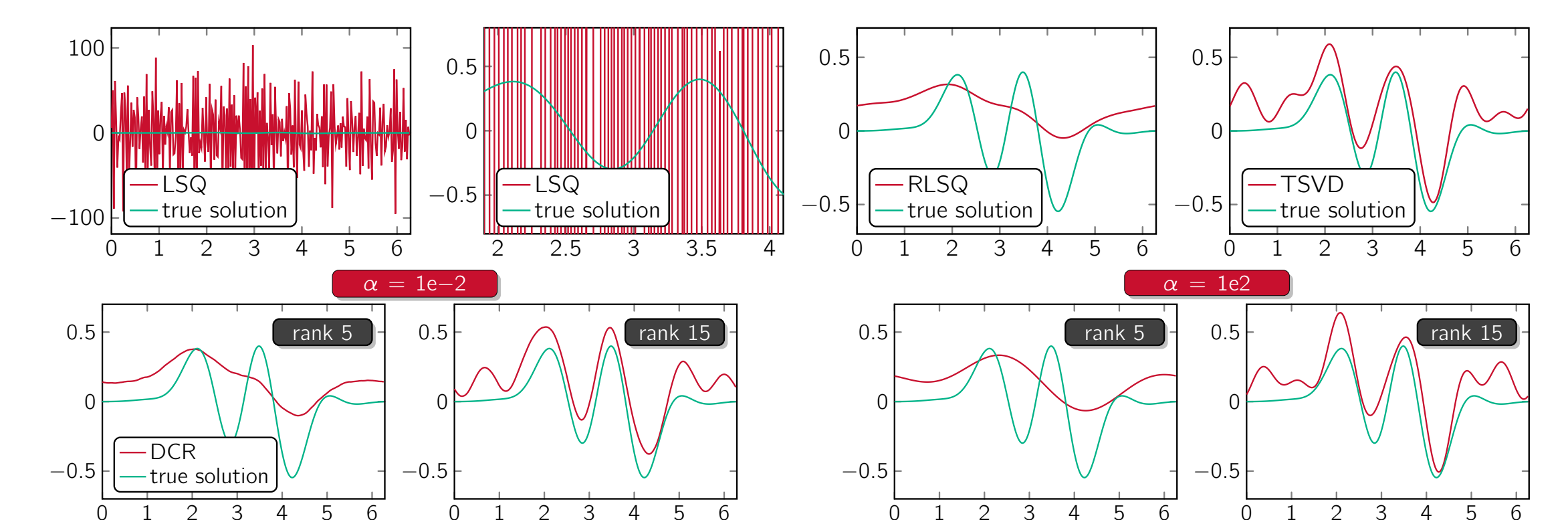


Figure 2: We report solutions for the least squares problem in (1) for different numerical strategies. The numerical solution is shown in red and the true solution \mathbf{x}_{true} is shown in green. Top row: For the unregularized case ($\alpha = 0$) we can observe that the noise is amplified; the computed solution has nothing to do with the true solution. For the regularized case (with regularization parameter $\alpha = 1\text{e}-2$ and regularization operator $\mathbf{L}^T \mathbf{L} = -\Delta$), we can see that we underfit the data. The best result is obtained by computing the solution through a low rank approximation $\mathbf{U}_r \mathbf{S}_r \mathbf{V}_r^T \approx \mathbf{A}$ (truncated SVD; we consider rank $r = 15$). Bottom row: We report results for the regularization operators $\mathbf{L}^T \mathbf{L} = \mathbf{I} - \mathbf{V}_r \mathbf{V}_r^T$ with regularization parameters $\alpha \in \{1\text{e}-2, 1\text{e}2\}$ and ranks $r \in \{5, 15\}$.

Conclusions

We have developed and tested a computational framework for solving and regularizing linear inverse problems [1]. We have tested a Thikonov-type regularization operator that is motivated from SVD and yields results that are consistent with the TSVD [2]. This regularization scheme outperforms standard regularization approaches based on the identity and Laplace operator. In our future work we aim at extending the proposed methodology to nonlinear inverse problems [5,6].

References

1. C. R. Vogel, Computational methods for inverse problems, SIAM, 2002.
2. J. Wittmer, B. Marin, & T. Bui-Thanh, A data-oriented statistical framework for inversion and imaging, AMS Madison, 2019.
3. J. Nocedal & S. Wright, Numerical Optimization, Springer Science, 1999.
4. A. Beck, Introduction to nonlinear optimization: Theory, algorithms, and applications with MATLAB, SIAM, 2014.
5. A. Mang & G. Biros: An inexact Newton–Krylov algorithm for constrained diffeomorphic image registration. SIAM Journal on Imaging Sciences 8(2):1030–1069, 2015.
6. A. Mang et al.: CLAIRE: A distributed-memory solver for constrained large deformation diffeomorphic image registration. SIAM Journal on Scientific Computing 41(5):C548–C584, 2019.